Scientia Iranica, Vol. 11, Nos. 1&2, pp 1 2

SCIENTIA
IRANICA

Prediction of Collapse Potential for Compacted Soils Using Artificial Neural Networks

G. Habibagahi* **and M. Taherian**[1]

Collapse, defined as the additional deformation of compacted soils when wetted, is believed to be responsible for damage to buildings resting on compacted fills, as well as failure in embankments and earth dams. In this paper, three different types of neural networks, namely, conventional Back-Propagation Neural Network (BPNN), Recurrent Neural Network (RNN) and Generalized Regression Neural Network (GRNN) are employed as computational tools to predict the amount of collapse and to investigate the influence of various parameters on the collapse potential. To arrive at this goal, 192 series of a single oedometer test were carried out on three soils with different initial conditions and inundated at different applied pressures. The test results were used to prepare the necessary database for training the neural network. Similar test results available in literature were also included in the database to arrive at a total of 330 sets of data. A comparison of the network prediction for collapse potential with some available models shows the superiority of the network in terms of the accuracy of prediction. Moreover, by analyzing the network connection weights, the relative importance of different parameters on collapse potential was assessed. Based on this analysis, for a given soil type, the initial dry unit weight, γ_d, is the most important factor influencing collapse potential.

INTRODUCTION

All soils settle upon loading. However, unsaturated soils may reduce in volume when inundated under constant applied pressure. The amount of this additional deformation, called "collapse", depends on several factors, such as applied pressure, water content, dry density, principal stress ratio, clay content and compaction method. The effective stress principle, used to describe the mechanical behavior of unsaturated soils, fails to predict the collapse phenomena. This fact was first indicated by Jennings anf Burland [1].

Collapse may occur in natural soils as well as in compacted fills and embankments, although the mechanism and contributing agents may differ. The influence of different parameters on the amount of collapse has been discussed by many investigators [2-6]. Collapse potential is assessed by different investigators employing different methods. These methods vary from simple empirical equations based on statistical regression [7,8] to experimental procedures, such as single and double oedometer tests, which have been described by Jennings and Knight [9] and Houston et al. [10], respectively.

Wetting induced collapse is believed to be responsible for failure in several earth dams [11,12], as well as damage to buildings resting on compacted soils, reported by Lawton et al. [13]. Despite the considerable amount of work done in this area, the functional relationship between various soil parameters and the amount of collapse deformation is not well established and the exact interrelationship is still a matter of speculation. The neural network, as a computational tool, has proved to be capable of establishing a relationship between a series of input data and the corresponding outputs, no matter how complex this relationship may be. Hence, this method is employed, in this paper, to investigate the collapse potential of unsaturated soils. In order to arrive at a robust neural network, a comprehensive database is required a priori. Therefore, the results of 192 oedometer tests performed in this study were used to serve as the required database. Furthermore, other similar data

*. *Corresponding Author, Department of Civil Engineering, Shiraz University, Shiraz, I.R. Iran.*
1. *Department of Civil Engineering, Shiraz University, Shiraz, I.R. Iran.*

available in the literature were included to arrive at a more comprehensive database. Next, the efficacy of the method was verified by comparing the predicted results with some of the existing empirical relationships.

NEURAL NETWORKS

A Neural Network (NN) is a computational method inspired by the neural operation of the human brain. The network "learns" from previous experience by adjusting the network's unknowns. Various types of neural network have been developed and have found their applications in different disciplines of engineering.

The Back-Propagation Neural Network (BPNN), has received attention in different engineering domains and, more recently, in geotechnical engineering. The works of Ghaboussi [14], Goh [15], Ellis et al. [16], Goh [17], Ghaboussi and Sidarta [18] and Habibagahi et al. [19] are typical examples of the application of the BPNN in geotechnical engineering. Besides BPNN, the application of other networks, such as the Recurrent Neural Network (RNN) and the Generalized Regression Neural Network (GRNN), have also been found in geotechnical engineering. Examples for the application of RNN and GRNN in geotechnical engineering include the works of Zhu et al. [20], Abu Kiefa [21] and Penumadu and Zhao [22].

In this paper, the three above-mentioned networks, namely, BPNN, RNN and GRNN were employed to assess the collapse potential of unsaturated soils. In the following sections, a brief description of each network is presented and interested readers are referred to available textbooks, such as Bose and Liang [23] and Haykin [24] for more details.

BPNN

A Back-Propagation Neural Network (BPNN) is comprised of three components: An architecture (arrangement of neurons in the network), an activation function and a learning rule. The architecture itself is comprised of three parts, namely, an input layer, an output layer and one or more hidden layers. Each layer consists of a number of neurons. All neurons of each layer are fully connected to the neurons of the next layer, but there is no connection between the neurons within the same layer. A weight is assigned to each connection and each neuron has an activation function, usually of the sigmoid type. The activation function of each neuron receives, as input, the weighted sum of all outputs from the previous layer and, in turn, outputs the result to the neurons of the next layer. Figure 1 indicates a block diagram for a BPNN. A learning rule is required to adjust the weights (unknowns) in the network, in order to minimize the difference between the network outputs

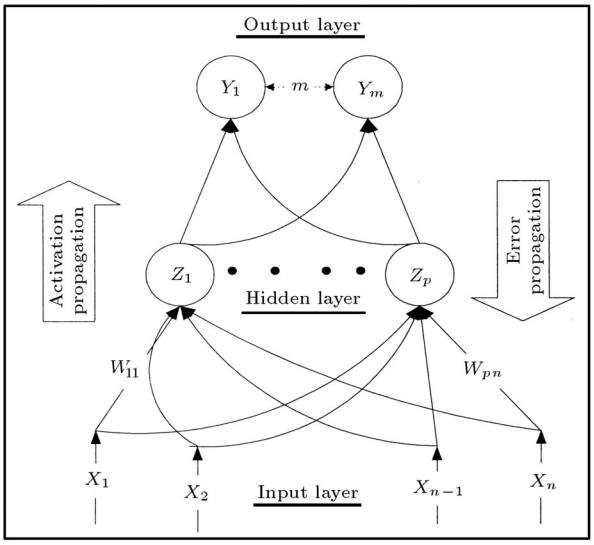

Figure 1. Block diagram for Back-Propagation Neural Network (BPNN).

and the target (desired) values. The back propagation algorithm, as described by Rumelhart et al. [25], is the most commonly used algorithm. In this algorithm, the summed square of the errors is calculated and back propagated through the network using a gradient-descent rule. This process is repeated and the connection weights are adjusted each time until the summed square of the errors is below an acceptable value. At this point, the network is said to be "trained". In order to check the performance of the network, it is a usual practice to test the network using some series of data (test patterns) that have not been presented to the network during the training process. It is a common practice to devote about 20% of the datasets present in the database for testing (validation) of the network.

RNN

Recurrent Neural Networks (RNN) are very similar to BPNN. They utilize the same kind of activation function and learning rule. However, the basic difference lies in the architecture or arrangement of neurons. In RNNs, outputs of hidden neurons are not only fed forward to the next layer but are also fed back to the input layer. Hence, additional neurons, equal in number to the hidden neurons, are assigned to the input layer. Figure 2 represents a block diagram for RNN.

GRNN

Generalized Regression Neural Network (GRNN) is based on the nonlinear regression theory and is a popular statistical tool for function approximation. Unlike BPNN and RNN, in GRNN, the training patterns are

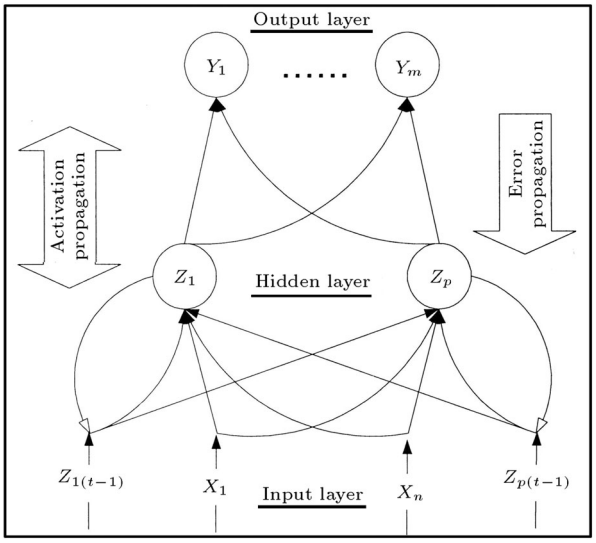

Figure 2. Block diagram for Recurrent Neural Network (RNN).

propagated through the network only once and, thus, the training is achieved very quickly. In its network form, GRNN is a four-layer network with one input layer, two hidden layers and one output layer. In the first hidden layer, also known as the pattern layer, one neuron is assigned for each training pattern (dataset) present in the database. These neurons have radial basis activation functions of the form:

$$h_i = e^{-D_i^2/(2\sigma^2)}, \tag{1}$$

where h_i is the output of neuron "i"; σ is a constant controlling size of the basis function also called "smoothing factor" and D_i is the Euclidean distance between the input vector and the center of the hidden neuron "i", given by:

$$D_i = \|x - u_i\| = \left[(x - u_i)^t (x - u_i)\right]^{0.5}, \tag{2}$$

where $\mathbf{x}$ is the input vector and $\mathbf{u}_i$ is the center of neuron "i".

The second hidden layer, also called the summation layer, performs a weighted sum of outputs from the previous layer. Figure 3 represents a GRNN block diagram for a network with one output neuron. Generally, GRNN is robust for approximating continuous functions. However, it may require a larger number of parameters than BPNN for the same degree of accuracy. Furthermore, it is possible to improve the accuracy of the model by adjusting the shape and size of the basis functions through replacing the Euclidean distance by the Mahalanobis distance, expressed by:

$$D_i = \left[(x - u_i)^t K (x - u_i)\right]^{0.5}, \tag{3}$$

where K is the inverse of the covariance matrix of input vectors, given by:

$$K = \left[E(x - m)(x - m)\right]^{-1}, \tag{4}$$

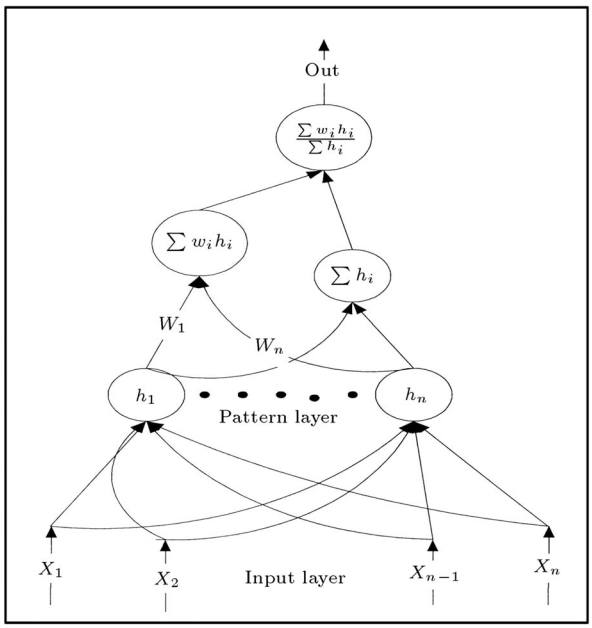

Figure 3. Block diagram for Generalized Regression Neural Network (GRNN).

where m is mean vector over all input vectors. Using this method, the hidden neuron output is given by:

$$h_i = e^{-D_i^2/2}. \tag{5}$$

Using the Mahalanobis distance, the basis function is no longer symmetric and the contours of the constant Mahalanobis distance define hyper-ellipsoids in the input space. In other words, the size and shape of the basis function are adjusted automatically to optimize partitioning of the input space and there is no need to determine the optimum smoothing factor as required by the first approach. Here, the latter method was employed to study the collapse potential.

EXPERIMENTATION

Neural networks need a large and comprehensive database both for training and testing phases. To achieve this goal, a large number of single oedometric tests were carried out on soil specimens prepared with different initial conditions. Details of the soil properties, preparation and testing method are given in the following sections.

Soil and Test Program

Bulk samples of soil were obtained from three locations at a site in Seavand, 65-km northeast of Shiraz City in the Fars province of Iran. Previous experience had revealed the collapsing nature of the soil [26]. Figure 4 shows the particle size distribution of the soils. A large number of oedometric tests (192 tests)

Table 1. Properties of tested soils.

Soil Series	Sand %	Silt %	Clay %	C_U	C_C	LL %	PI %	G_s
A	13.0	75.0	12.0	16.7	1.4	22.6	5.0	2.68
B	32.0	52.0	16.0	50.0	1.8	24.2	8.0	2.68
C	35.0	52.0	13.0	35.0	2.4	28.2	3.0	2.68

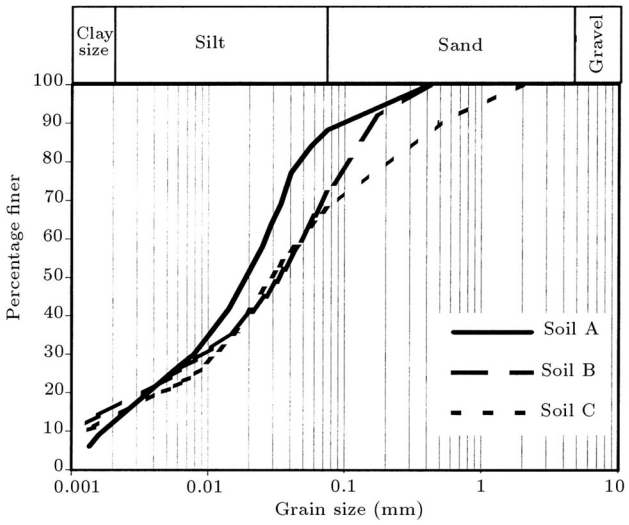

Figure 4. Grain size distribution of the soils tested.

were conducted and the amount of collapse was measured under different initial conditions and at different applied stresses. The general characteristics of the soils are presented in Table 1. The method of sample preparation and the test procedure are subsequently described.

Sample Preparation

To prepare samples for the oedometer test, soil, having a certain amount of water content, was compacted into the consolidation ring. The ring was placed into a prefabricated mold that made it possible to compact the soil into the consolidation ring using a standard proctor hammer. The hammer blows were applied on a metal pad resting on top of the soil, in order to provide relatively uniform compaction of the soil into the consolidation ring.

Samples with different initial conditions were obtained by varying the number of blows and/or water content. Table 2 shows the initial conditions of the samples prepared using the aforementioned procedure.

Testing Method

Single oedometer collapse tests were conducted on all samples. For this purpose, each specimen was placed between two porous stones in a conventional floating type oedometer apparatus. To minimize any change in water content during the tests, the top of the oedometer box was covered using a plastic sheet fixed with a rubber ring. A seating pressure of 20 kPa was applied and the load was doubled when the monitored dial gauge reading versus time became asymptotic. At a predetermined pressure the sample was inundated with distilled water and the amount of collapse was measured.

Test Results

A total of 192 single oedometer collapse tests were performed on soil samples with initial dry densities varying from 1.23 Mg/m^3 to 1.91 Mg/m^3 and initial water content, which was varied from 4.9% to 16.9%. Collapse was measured at inundation pressures of 100, 200, 400 and 800 kPa. Typical test results are shown in Figure 5. Values of the collapse potential, determined from the test results, are given in Table 3. There are different equations cited in literature for defining collapse potential. Luttengger and Saber [27] presented a summary of these equations proposed by different investigators. The term, "collapse potential", used in this study, is defined as the ratio of the change in the specimen height upon inundation to its initial height before loading. Note that for several tests, no collapse was observed.

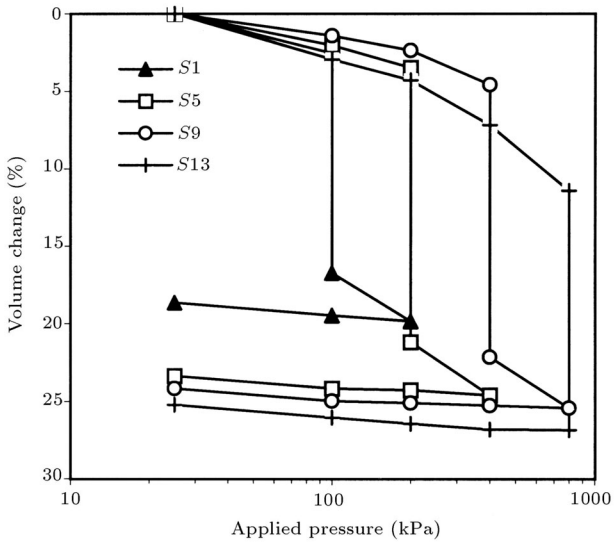

Figure 5. Typical oedometric test results.

Table 2. Details of tested specimens.

Soil Series	Soil Specimens	Initial Water Content (%)	Initial Dry Density (Mg/m^3)	Applied Pressure at Wetting (kPa)
A	S1, S2, S3, S4	4.9	1.36, 1.47, 1.56, 1.64	100
A	S5, S6, S7, S8	5.3	1.30, 1.45, 1.50, 1.66	200
A	S9, S10, S11, S12	6.0	1.32, 1.42, 1.52, 1.61	400
A	S13, S14, S15, S16	5.8	1.30, 1.42, 1.55, 1.61	800
A	S17, S18, S19, S20	9.4	1.23, 1.48, 1.61, 1.73	100
A	S21, S22, S23, S24	9.7	1.28, 1.45, 1.55, 1.72	200
A	S25, S26, S27, S28	9.3	1.24, 1.43, 1.54, 1.68	400
A	S29, S30, S31, S32	9.2	1.24, 1.42, 1.53, 1.69	800
A	S33, S34, S35, S36	12.5	1.32, 1.54, 1.62, 1.84	100
A	S37, S38, S39, S40	11.6	1.28, 1.41, 1.54, 1.70	200
A	S41, S42, S43, S44	12.4	1.25, 1.39, 1.53, 1.69	400
A	S45, S46, S47, S48	12.1	1.26, 1.43, 1.50, 1.68	800
A	S49, S50, S51, S52	15.7	1.40, 1.50, 1.65, 1.84	100
A	S53, S54, S55, S56	15.6	1.25, 1.37, 1.48, 1.55	200
A	S57, S58, S59, S60	15.6	1.28, 1.35, 1.50, 1.56	400
A	S61, S62, S63, S64	16.3	1.25, 1.34, 1.50, 1.58	800
B	S65, S66, S67, S68	5.4	1.36, 1.44, 1.56, 1.65	100
B	S69, S70, S71, S72	6.1	1.34, 1.44, 1.54, 1.62	200
B	S73, S74, S75, S76	5.0	1.38, 1.49, 1.57, 1.65	400
B	S77, S78, S79, S80	5.5	1.38, 1.48, 1.54, 1.62	800
B	S81, S82, S83, S84	9.2	1.32, 1.46, 1.62, 1.72	100
B	S85, S86, S87, S88	9.1	1.35, 1.50, 1.60, 1.73	200
B	S89, S90, S91, S92	8.4	1.36, 1.49, 1.65, 1.75	400
B	S93, S94, S95, S96	9.1	1.36, 1.46, 1.57, 1.72	800
B	S97, S98, S99, S100	12.4	1.30, 1.45, 1.55, 1.77	100
B	S101, S102, S103, S104	12.4	1.32, 1.44, 1.60, 1.77	200
B	S105, S106, S107, S108	12.4	1.33, 1.40, 1.51, 1.74	400
B	S109, S110, S111, S112	12.4	1.30, 1.41, 1.58, 1.69	800
B	S113, S114, S115, S116	16.9	1.40, 1.52, 1.59, 1.75	100
B	S117, S118, S119, S120	16.9	1.34, 1.47, 1.60, 1.75	200
B	S121, S122, S123, S124	16.9	1.34, 1.51, 1.62, 1.80	400
B	S125, S126, S127, S128	16.9	1.37, 1.47, 1.61, 1.77	800
C	S129, S130, S131, S132	6.0	1.45, 1.57, 1.64, 1.77	100
C	S133, S134, S135, S136	6.0	1.45, 1.57, 1.67, 1.79	200
C	S137, S138, S139, S140	6.0	1.42, 4.53, 1.67, 1.78	400
C	S141, S142, S143, S144	6.0	1.48, 1.59, 1.66, 1.80	800
C	S145, S146, S147, S148	9.3	1.43, 1.58, 1.75, 1.91	100
C	S149, S150, S151, S152	9.3	1.40, 1.60, 1.75, 1.89	200
C	S153, S154, S155, S156	9.3	1.36, 1.52, 1.65, 1.75	400
C	S157, S158, S159, S160	9.3	1.41, 1.51, 1.61, 1.72	800

Table 2. Continued.

Soil Series	Soil Specimens	Initial Water Content (%)	Initial Dry Density (Mg/m^3)	Applied Pressure at Wetting (kPa)
C	S161, S162, S163, S164	12.2	1.50, 1.57, 1.73, 1.90	100
C	S165, S166, S167, S168	12.2	1.45, 1.58, 1.68, 1.85	200
C	S169, S170, S171, S172	12.2	1.46, 1.57, 1.69, 1.88	400
C	S173, S174, S175, S176	12.2	1.45, 1.54, 1.70, 1.84	800
C	S177, S178, S179, S180	15.7	1.52, 1.65, 1.71, 1.78	100
C	S181, S182, S183, S184	15.7	1.45, 1.63, 1.70, 1.77	200
C	S185, S186, S187, S188	15.7	1.46, 1.55, 1.65, 1.74	400
C	S189, S190, S191, S192	15.7	1.44, 1.58, 1.70, 1.76	800

NEURAL NETWORK ANALYSIS

Network Architecture

As mentioned earlier, three types of neural network (Back-Propagation Neural Network (BPNN), Recurrent Neural Network (RNN) and Generalized Regression Neural Network (GRNN)) were used in this study. All the networks had ten input neurons and one output neuron. The ten input neurons represent sand content, silt content, clay content, coefficient of uniformity, coefficient of curvature, liquid limit, plasticity index, initial water content, initial dry density and the applied pressure before inundation. The input values for the applied pressure were expressed in logarithmic form, since it was found that this substantially improves the networks' training process. The output layer had a single neuron to represent the amount of collapse potential.

A single hidden layer was adopted for BPNN and RNN. Currently, there is no rule to determine the optimum number of hidden neurons. However, there are two approaches to arrive at the optimum number of hidden neurons. The first approach starts with a network with a large number of hidden neurons and then "pruning" the network by reducing the number of hidden neurons to arrive at the final network architecture. The second approach, on the contrary, starts with a network with a minimal number of neurons in the hidden layer and increases the network size in steps by adding a single hidden neuron each time and examining the network performance. This process is continued until there is no further improvement in the network performance. In this study, the latter approach was adopted to determine the number of hidden neurons. Based on this approach, a network with six neurons had the best performance for the back-propagation type network, BPNN6 and a network with four neurons had the best performance for the recurrent type network, RNN4. As mentioned before, GRNN has a fixed number of neurons in the hidden layer, equal in number to the number of training datasets present in the database.

Database

A powerful network needs a comprehensive database to cover a wide variety of soil types with different initial conditions. Such a network will be capable of predicting collapse potential with good accuracy, not only for the training patterns (training datasets) but also, for the patterns that the network had not been exposed to during the training process (validation or generalization property). To arrive at this goal, an attempt was made to increase the amount of data in the database by adding data that were available in the literature, based on similar test procedures.

A total of 138 sets of data from test results performed on eight different soils and reported by Basma and Tuncer [7], were added to the database to arrive at a total of 330 sets of data. The properties of these soils and the corresponding oedometer test results are given in Tables 4 and 5, respectively.

The percentage collapse potentials given in Table 5 were interpreted from the graphs provided by Basma and Tuncer [7] and, hence, had a limited accuracy (resolution in reading percentage of collapse potential: $\pm$ 0.1). Moreover, in the experimental procedure reported by Basma and Tuncer [7], a seating pressure of 5 kPa was used compared to the 20 kPa seating pressure adopted in the present experimental program. Hence, an adjustment was made to the initial dry densities of the specimens prepared in this study by extrapolating the corresponding e-log P curves.

From a total of 330 sets of data, 264 sets were used for training the network. The remaining 66 sets of data were used to test the network. Testing and training datasets are indicated in Tables 3 and 5.

Performance of Neural Networks

Network performance may be evaluated, quantitatively, in terms of coefficient of correlation (R^2), mean

Table 3. Oedometric test results.

Sample No.	Initial Water Content: %	Initial Dry Unit Weight: kN/m^3	Pressure at Wetting: kPa	Collapse Potential: %	NN Pattern Type
S1	4.9	13.64	100	14.1	Training
S2	4.9	14.72	100	8.1	Training
S3	4.9	15.60	100	4.2	Training
S4	4.9	16.48	100	3.9	Training
S5	5.3	13.15	200	17.3	Testing
S6	5.3	14.62	200	11.6	Training
S7	5.3	15.21	200	8.2	Training
S8	5.3	16.68	200	6.3	Training
S9	6.0	13.44	400	17.1	Training
S10	6.0	14.32	400	13.5	Testing
S11	6.0	15.30	400	9.0	Training
S12	6.0	16.28	400	6.1	Training
S13	5.8	13.14	800	15.2	Training
S14	5.8	14.42	800	14.6	Training
S15	5.8	15.60	800	11.3	Testing
S16	5.8	16.19	800	9.3	Training
S17	9.4	12.56	100	17.6	Training
S18	9.4	14.91	100	4.5	Training
S19	9.4	16.28	100	1.7	Training
S20	9.4	17.46	100	0.0	Testing
S21	9.7	12.85	200	17.6	Training
S22	9.7	14.62	200	8.7	Training
S23	9.7	15.60	200	3.7	Training
S24	9.7	17.27	200	0.4	Training
S25	9.3	12.56	400	11.2	Testing
S26	9.3	14.52	400	11.4	Training
S27	9.3	15.50	400	6.4	Training
S28	9.3	16.97	400	1.0	Training
S29	9.2	12.56	800	10.9	Training
S30	9.2	14.32	800	13.3	Testing
S31	9.2	15.60	800	7.7	Training
S32	9.2	16.97	800	4.1	Training
S33	12.5	13.44	100	13.9	Training
S34	12.5	15.60	100	1.9	Training
S35	12.5	16.38	100	0.2	Testing
S36	12.5	18.54	100	0.0	Training
S37	11.6	13.05	200	14.1	Training
S38	11.6	14.22	200	11.3	Training
S39	11.6	15.60	200	5.5	Training
S40	11.6	17.17	200	0.3	Testing

Table 3. Continued.

Sample No.	Initial Water Content: %	Initial Dry Unit Weight: kN/m^3	Pressure at Wetting: kPa	Collapse Potential: %	NN Pattern Type
S41	12.4	12.65	400	11.0	Training
S42	12.4	14.03	400	11.2	Training
S43	12.4	15.50	400	4.8	Training
S44	12.4	17.07	400	0.4	Training
S45	12.1	12.85	800	5.6	Testing
S46	12.1	14.52	800	7.4	Training
S47	12.1	15.21	800	6.4	Training
S48	12.1	16.97	800	2.4	Training
S49	15.7	14.03	100	10.4	Training
S50	15.7	15.01	100	5.2	Testing
S51	15.7	16.59	100	0.1	Training
S52	15.7	18.44	100	0.0	Training
S53	14.6	12.65	200	9.0	Training
S54	14.6	13.83	200	9.3	Training
S55	14.6	14.91	200	7.4	Testing
S56	14.6	15.60	200	4.7	Training
S57	15.6	12.75	400	4.6	Training
S58	15.6	13.54	400	4.9	Training
S59	15.6	15.11	400	5.1	Training
S60	15.6	15.70	400	4.5	Testing
S61	16.3	12.66	800	0.6	Training
S62	16.3	13.54	800	1.3	Training
S63	16.3	15.01	800	0.3	Training
S64	16.3	15.89	800	0.2	Training
S65	5.4	13.54	100	10.4	Testing
S66	5.4	14.32	100	8.2	Training
S67	5.4	15.50	100	2.1	Training
S68	5.4	16.38	100	2.9	Training
S69	6.1	13.54	200	13.0	Training
S70	6.1	14.32	200	10.0	Testing
S71	6.1	15.31	200	7.1	Training
S72	6.1	16.09	200	5.1	Training
S73	5.0	13.73	400	14.3	Training
S74	5.0	14.81	400	11.2	Training
S75	5.0	15.60	400	8.4	Testing
S76	5.0	16.38	400	8.3	Training
S77	5.5	13.73	800	13.2	Training
S78	5.5	14.72	800	12.7	Training
S79	5.5	15.30	800	11.1	Training
S80	5.5	16.09	800	12.5	Testing

Table 3. Continued.

Sample No.	Initial Water Content: %	Initial Dry Unit Weight: kN/m^3	Pressure at Wetting: kPa	Collapse Potential: %	NN Pattern Type
S81	9.2	13.15	100	15.0	Training
S82	9.2	14.81	100	5.5	Training
S83	9.2	16.19	100	0.7	Training
S84	9.2	17.17	100	0.0	Training
S85	9.1	13.54	200	15.0	Testing
S86	9.1	15.01	200	9.0	Training
S87	9.1	15.99	200	0.2	Training
S88	9.1	17.27	200	0.4	Training
S89	8.4	13.54	400	14.4	Training
S90	8.4	14.81	400	11.4	Testing
S91	8.4	16.38	400	3.8	Training
S92	8.4	17.27	400	1.2	Training
S93	9.1	13.64	800	11.1	Training
S94	9.1	14.62	800	11.1	Training
S95	9.1	15.70	800	8.0	Testing
S96	9.1	17.17	800	2.1	Training
S97	12.4	13.15	100	14.3	Training
S98	12.4	14.62	100	9.3	Training
S99	12.4	15.60	100	0.0	Training
S100	12.4	17.76	100	0.1	Testing
S101	12.4	13.34	200	10.5	Training
S102	12.4	14.52	200	5.6	Training
S103	12.4	16.09	200	1.4	Training
S104	12.4	17.76	200	0.1	Training
S105	12.4	13.44	400	10.1	Testing
S106	12.4	14.03	400	9.9	Training
S107	12.4	15.21	400	6.6	Training
S108	12.4	17.46	400	0.2	Training
S109	12.4	13.05	800	8.1	Training
S110	12.4	14.22	800	9.1	Testing
S111	12.4	15.99	800	5.1	Training
S112	12.4	16.87	800	1.4	Training
S113	16.9	14.13	100	10.8	Training
S114	16.9	15.03	100	7.0	Training
S115	16.9	15.99	100	1.1	Testing
S116	16.9	17.56	100	0.0	Training
S117	16.9	13.54	200	12.4	Training
S118	16.9	14.81	200	8.9	Training
S119	16.9	16.09	200	3.4	Training
S120	16.9	17.56	200	0.0	Testing

Table 3. Continued.

Sample No.	Initial Water Content: %	Initial Dry Unit Weight: kN/m^3	Pressure at Wetting: kPa	Collapse Potential: %	NN Pattern Type
S121	16.9	13.54	400	5.0	Training
S122	16.9	15.21	400	5.4	Training
S123	16.9	16.28	400	2.4	Training
S124	16.9	18.05	400	0.0	Training
S125	16.9	13.83	800	0.1	Testing
S126	16.9	14.72	800	1.3	Training
S127	16.9	16.19	800	0.1	Training
S128	16.9	17.76	800	0.0	Training
S129	6.0	14.42	100	10.9	Training
S130	6.0	15.60	100	6.8	Testing
S131	6.0	16.28	100	2.9	Training
S132	6.0	17.60	100	0.8	Training
S133	6.0	14.42	200	13.8	Training
S134	6.0	15.60	200	8.5	Training
S135	6.0	16.58	200	4.3	Testing
S136	6.0	17.76	200	1.7	Training
S137	6.0	14.13	400	13.6	Training
S138	6.0	15.21	400	12.2	Training
S139	6.0	16.58	400	6.2	Training
S140	6.0	17.66	400	2.6	Testing
S141	6.0	14.72	800	13.0	Training
S142	6.0	15.79	800	12.6	Training
S143	6.0	16.48	800	7.0	Training
S144	6.0	17.85	800	5.4	Training
S145	9.2	14.22	100	4.7	Testing
S146	9.2	15.70	100	1.8	Training
S147	9.2	17.37	100	0.0	Training
S148	9.2	18.93	100	0.0	Training
S149	9.2	13.93	200	13.4	Training
S150	9.2	15.99	200	5.4	Testing
S151	9.2	17.37	200	0.5	Training
S152	9.2	18.74	200	0.0	Training
S153	9.2	13.54	400	7.4	Training
S154	9.2	15.11	400	8.4	Training
S155	9.2	16.38	400	5.6	Testing
S156	9.2	17.36	400	0.9	Training
S157	9.2	14.13	800	4.5	Training
S158	9.2	15.21	800	5.3	Training
S159	9.2	15.99	800	5.5	Training
S160	9.2	17.17	800	3.3	Testing

Table 3. Continued.

Sample No.	Initial Water Content: %	Initial Dry Unit Weight: kN/m^3	Pressure at Wetting: kPa	Collapse Potential: %	NN Pattern Type
S161	12.2	14.91	100	10.1	Training
S162	12.2	15.70	100	6.4	Training
S163	12.2	17.27	100	0.0	Training
S164	12.2	18.93	100	0.0	Training
S165	12.2	14.52	200	5.5	Testing
S166	12.2	15.79	200	5.2	Training
S167	12.2	16.78	200	0.0	Training
S168	12.2	18.44	200	0.0	Training
S169	12.2	14.62	400	5.0	Training
S170	12.2	15.70	400	3.6	Testing
S171	12.2	16.87	400	2.0	Training
S172	12.2	18.74	400	0.0	Training
S173	12.2	14.52	800	1.5	Training
S174	12.2	15.40	800	2.3	Training
S175	12.2	16.97	800	2.3	Testing
S176	12.2	18.34	800	0.3	Training
S177	15.7	15.30	100	1.7	Training
S178	15.7	16.58	100	0.0	Training
S179	15.7	17.17	100	0.0	Training
S180	15.7	17.85	100	0.0	Testing
S181	15.7	14.62	200	0.9	Training
S182	15.7	16.38	200	0.3	Training
S183	15.7	17.07	200	0.1	Training
S184	15.7	17.76	200	0.0	Training
S185	15.7	14.72	400	0.1	Testing
S186	15.7	15.60	400	0.1	Training
S187	15.7	16.58	400	0.0	Training
S188	15.7	17.46	400	0.0	Training
S189	15.7	14.52	800	0.0	Training
S190	15.7	15.89	800	0.0	Testing
S191	15.7	17.07	800	0.0	Training
S192	15.7	17.66	800	0.0	Training

Table 4. Properties of soils tested by Basma and Tuncer [7].

Soil Series	Sand: %	Silt: %	Clay: %	C_u	C_C	LL: %	PI: %	G_s
S1	40.6	50.5	8.9	17.5	7.2	36.6	12.7	2.74
S2	47.8	47.2	5.0	25.0	1.1	29.1	11.2	2.72
S3	13.3	73.5	13.2	60.0	15.0	57.2	28.9	2.69
S4	19.6	70.4	10.0	11.5	2.9	28.0	7.0	2.77
S5	24.4	49.6	26.0	35.0	0.5	36.0	11.1	2.66
S6	42.1	42.9	15.0	100.0	0.9	28.2	10.6	2.69
S7	84.0	7.0	9.0	6.4	1.6	30.0	3.0	2.63
S8	92.2	5.8	2.0	3.4	1.1	25.0	5.0	2.65

Table 5. Results of oedometric collapse tests reported by Basma and Tuncer [7].

Soil Series	Initial Water Content: %	Initial Dry Unit Weight: kN/m^3	Pressure at Wetting: kPa	Collapse Potential: %	NN Pattern Type
S1	4.0	15.0	400	12.5	Training
S1	6.0	15.0	400	10.1	Training
S1	8.0	15.0	400	12.5	Testing
S1	12.0	15.0	400	11.9	Training
S1	16.0	15.0	400	9.1	Training
S1	20.0	15.0	400	7.5	Training
S1	6.0	13.1	400	14.4	Training
S1	6.0	14.0	400	13.2	Testing
S1	6.0	15.0	400	10.2	Training
S1	6.0	15.9	400	7.8	Training
S1	6.0	16.8	400	4.2	Training
S1	6.0	17.8	400	1.3	Training
S1	6.0	18.7	400	0.0	Testing
S1	6.0	15.0	200	7.1	Training
S1	6.0	15.0	400	12.7	Training
S1	6.0	15.0	800	15.0	Training
S1	6.0	15.0	1600	15.6	Training
S1	6.0	15.0	3200	15.8	Testing
S2	4.0	15.4	400	14.8	Training
S2	6.0	15.4	400	13.3	Training
S2	8.0	15.4	400	11.7	Training
S2	12.0	15.4	400	8.7	Training
S2	16.0	15.4	400	5.0	Testing
S2	20.0	15.4	400	0.1	Training
S2	6.0	13.5	400	21.3	Training
S2	6.0	14.5	400	18.7	Training
S2	6.0	15.4	400	13.6	Training
S2	6.0	16.4	400	9.6	Testing
S2	6.0	17.4	400	6.0	Training
S2	6.0	18.3	400	1.0	Training
S2	6.0	19.3	400	0.0	Training
S2	6.0	15.4	200	8.5	Training
S2	6.0	15.4	400	13.6	Testing
S2	6.0	15.4	800	14.7	Training
S2	6.0	15.4	1200	17.5	Training
S2	6.0	15.4	3600	17.9	Training
S3	4.0	13.6	400	19.2	Training
S3	6.0	13.6	400	17.5	Testing
S3	8.0	13.6	400	16.2	Training
S3	12.0	13.6	400	15.0	Training

Table 5. Continued.

Soil Series	Initial Water Content: %	Initial Dry Unit Weight: kN/m^3	Pressure at Wetting: kPa	Collapse Potential: %	NN Pattern Type
S3	16.0	13.6	400	13.2	Training
S3	20.0	13.6	400	12.0	Training
S3	6.0	11.9	400	22.7	Testing
S3	6.0	12.8	400	20.0	Training
S3	6.0	13.6	400	17.5	Training
S3	6.0	14.5	400	9.5	Training
S3	6.0	15.3	400	6.3	Training
S3	6.0	16.2	400	3.3	Testing
S3	6.0	17.0	400	0.1	Training
S3	6.0	13.6	200	12.0	Training
S3	6.0	13.6	400	17.5	Training
S3	6.0	13.6	800	19.0	Training
S3	6.0	13.6	1600	21.6	Testing
S3	6.0	13.6	3200	21.9	Training
S4	4.0	13.8	400	16.8	Training
S4	8.0	13.8	400	15.1	Training
S4	12.0	13.8	400	14.3	Training
S4	16.0	13.8	400	7.0	Testing
S4	20.0	13.8	400	9.7	Training
S4	6.0	12.0	400	21.3	Training
S4	6.0	12.9	400	19.5	Training
S4	6.0	13.8	400	16.6	Testing
S4	6.0	14.6	400	12.0	Training
S4	6.0	15.5	400	7.5	Training
S4	6.0	16.3	400	5.2	Training
S4	6.0	17.2	400	3.7	Training
S4	6.0	13.8	200	12.0	Testing
S4	6.0	13.8	400	16.5	Training
S4	6.0	13.8	800	15.1	Training
S4	6.0	13.8	1600	20.8	Training
S4	6.0	13.8	3200	23.0	Training
S5	4.0	13.0	400	22.6	Testing
S5	6.0	13.0	400	21.1	Training
S5	8.0	13.0	400	19.3	Training
S5	12.0	13.0	400	19.2	Training
S5	16.0	13.0	400	14.9	Training
S5	20.0	13.0	400	11.0	Testing
S5	6.0	11.4	400	23.2	Training
S5	6.0	12.2	400	24.1	Training
S5	6.0	13.0	400	22.2	Training

Table 5. Continued.

Soil Series	Initial Water Content: %	Initial Dry Unit Weight: kN/m^3	Pressure at Wetting: kPa	Collapse Potential: %	NN Pattern Type
S5	6.0	13.9	400	16.1	Training
S5	6.0	14.7	400	15.8	Testing
S5	6.0	15.5	400	11.9	Training
S5	6.0	13.0	200	17.0	Training
S5	6.0	13.0	400	22.0	Training
S5	6.0	13.0	800	21.2	Testing
S5	6.0	13.0	1600	23.2	Training
S5	6.0	13.0	3200	24.5	Training
S6	4.0	14.6	400	24.5	Training
S6	6.0	14.6	400	22.5	Training
S6	8.0	14.6	400	18.6	Testing
S6	12.0	14.6	400	16.3	Training
S6	16.0	14.6	400	16.0	Training
S6	20.0	14.6	400	14.0	Training
S6	6.0	12.8	400	26.4	Training
S6	6.0	13.7	400	25.1	Testing
S6	6.0	14.6	400	20.2	Training
S6	6.0	15.6	400	16.5	Training
S6	6.0	16.5	400	16.1	Training
S6	6.0	17.4	400	9.4	Training
S6	6.0	18.3	400	9.0	Testing
S6	6.0	14.6	200	14.9	Training
S6	6.0	14.6	400	19.9	Training
S6	6.0	14.6	800	23.0	Training
S6	6.0	14.6	1600	25.7	Training
S6	6.0	14.6	3200	26.4	Testing
S7	6.0	18.2	200	0.0	Training
S7	6.0	18.2	400	0.1	Training
S7	6.0	18.2	800	0.1	Training
S7	6.0	18.2	1600	1.5	Training
S7	6.0	18.2	3200	4.2	Testing
S7	3.0	18.2	400	1.2	Training
S7	6.0	18.2	400	0.0	Training
S7	9.0	18.2	400	0.0	Training
S7	12.0	18.2	400	0.0	Testing
S7	6.0	15.7	400	6.6	Training
S7	6.0	16.3	400	4.3	Training
S7	6.0	17.7	400	1.0	Training
S7	6.0	18.2	400	0.0	Training
S7	6.0	19.2	400	0.0	Testing

Table 5. Continued.

Soil Series	Initial Water Content: %	Initial Dry Unit Weight: kN/m^3	Pressure at Wetting: kPa	Collapse Potential: %	NN Pattern Type
S8	6.0	16.9	200	0.0	Training
S8	6.0	16.9	400	0.9	Training
S8	6.0	16.9	800	2.1	Training
S8	6.0	16.9	1600	3.1	Training
S8	6.0	16.9	3200	6.5	Testing
S8	0.0	16.9	400	2.7	Training
S8	3.0	16.9	400	1.0	Training
S8	6.0	16.9	400	0.5	Training
S8	9.0	16.9	400	0.0	Training
S8	12.0	16.9	400	0.0	Testing
S8	6.0	14.6	400	6.0	Training
S8	6.0	15.1	400	5.1	Training
S8	6.0	16.4	400	2.1	Training
S8	6.0	16.9	400	1.0	Training
S8	6.0	17.8	400	0.0	Testing

summed square of the errors (MSSE) and the error rate. Error rate was defined by Yeh et al. [28] as:

$$\text{Error Rate} = \frac{1}{N_p}\sum_{i=1}^{N_p}\text{error}_i, \tag{6}$$

where:

$$\text{error}_i = \sqrt{\sum_{J=1}^{N_{\text{OUT}}}(T_J - O_J)^2/N_{\text{OUT}}}, \tag{7}$$

where T, O = target and network output values, respectively, N_p= number of input patterns and N_{out} = number of neurons in the output layer. For a network with one output neuron, as in this study, Equation 6 reduces to:

$$\text{Error Rate} = \sum_{i=1}^{N_p}\Big|(T_i - O_i)\Big|/N_p. \tag{8}$$

These three indices were used to assess and compare the performance of the different neural networks studied. The results for BPNN6, RNN4 and GRNN are given in Table 6. From this table, it is clear that BPNN6 had the best performance in predicting the testing datasets, while GRNN had the best performance for the training datasets. Generalization capability is of utmost importance in any modeling technique. BPNN6 showed the best prediction capability for testing datasets (best generalization capability), also presenting a reasonable performance for the training datasets. Therefore, BPNN6 was selected as the superior network for assessing the collapse potential of unsaturated soils.

Neural Network Results

Figure 6 indicates the network architecture of the selected neural network, BPNN6. The training performance of the network is shown in Figure 7. As shown in this figure, the network was trained after 150,000 epochs, where the network error no longer decreased.

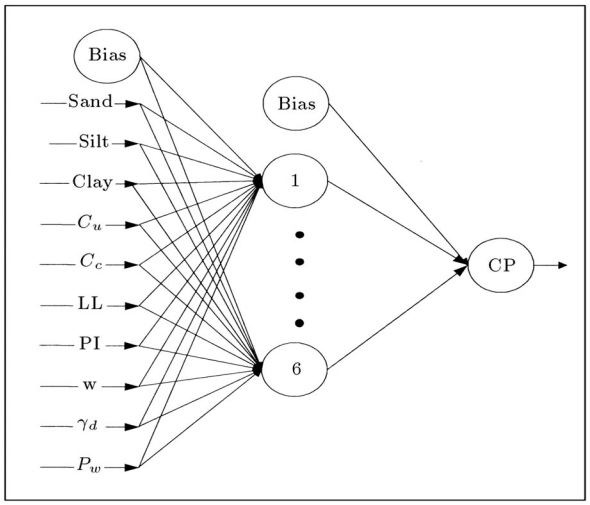

Figure 6. Architecture of neural network used to predict collapse potential.

Table 6. Summary of performance indices.

	BPNN		RNN		GRNN		Eq. 9	Eq. 10
	Training	Testing	Training	Testing	Training	Testing		
Coefficient of Correlation (R^2)	0.97	0.95	0.96	0.93	0.98	0.92	0.75	0.68
Mean Sum Square of Error (MSSE)	1.32	2.42	1.78	3.51	0.98	3.41	16.6	22.4
Error Rate	0.86	1.01	1.03	1.41	0.73	1.42	2.95	3.67

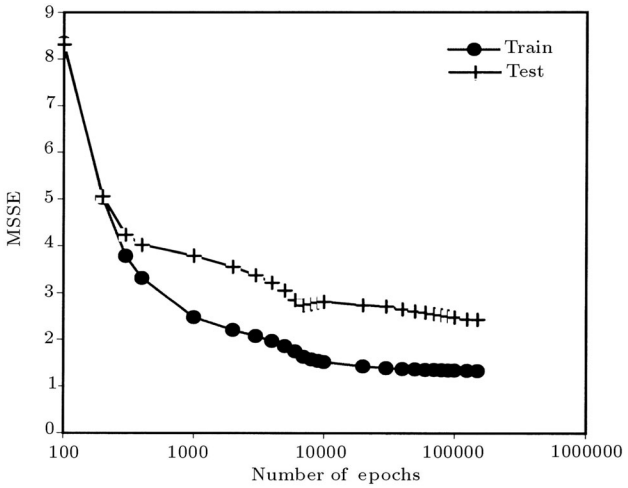

Figure 7. Performance of the network during training.

Each epoch is defined as one cycle of presentation of all training datasets to the network.

"Overtraining" (overfitting) may occur if a network is trained excessively, at which point, the network starts to learn "noise" contained in the training datasets. Beyond this point, although the network's training error may continue to decline, the testing error increases rapidly. In order to guard against overtraining, the network was examined during the training process by monitoring its performance for the testing records. The results are also shown in Figure 7. As indicated in this figure, there is an almost continuous reduction in the mean sum squared of errors for testing records during the training process and, hence, no overfitting had occurred.

The weight matrix of the trained network, BPNN6, is given in Table 7. Figure 8 shows the network prediction for collapse potential compared with the actual measured values. As described in the section dealing with testing method and sample preparation procedure, the method adopted in this study utilized a standard proctor hammer to compact the soil into the consolidation mold. This procedure

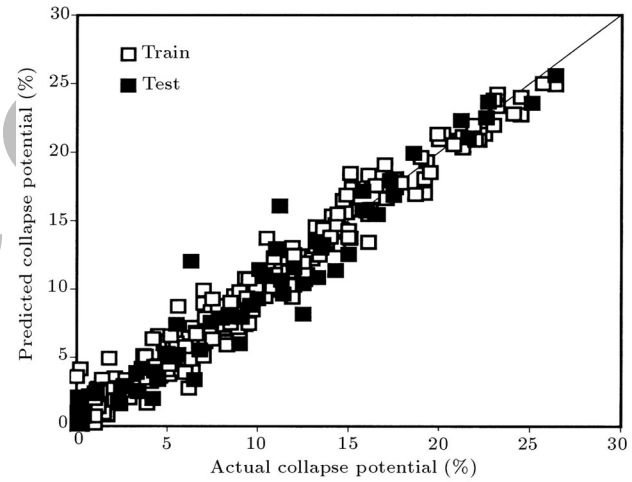

Figure 8. Prediction of neural network (BPNN6) versus actual measured values.

Table 7. Connection weights of the BPNN6 and Relative Importance (RI) of input parameters.

Hidden Neuron	Sand	Silt	Clay	C_u	C_C	LL	PI	w	γ_d	P_w	Input Bias	Output
1	-0.216	-0.024	0.213	-0.218	0.109	0.109	0.275	-0.099	0.241	-0.042	0.490	0.305
2	0.104	0.077	0.115	-0.155	0.086	0.086	0.038	0.234	0.262	-0.080	0.121	-0.110
3	1.038	0.473	-0.104	-0.234	-0.049	-0.049	-0.280	0.797	-0.316	-0.335	-0.007	-0.158
4	0.584	0.576	-0.364	-0.376	-0.637	-0.637	0.531	0.209	0.164	-0.501	0.209	-0.219
5	0.287	0.052	0.243	0.036	-0.077	-0.077	0.026	0.397	0.118	-0.264	0.156	-0.174
6	0.033	0.368	-0.383	-0.002	0.202	0.202	-0.392	0.958	-0.146	-0.370	-0.104	0.429
Bias	-	-	-	-	-	-	-	-	-	-	-	0.500
R.I. (%)	7.48	6.47	8.84	10.18	5.43	15.04	13.90	8.55	15.32	8.72	-	-

was different for the records obtained by Basma and Tancer [7], where static compaction was employed to prepare the samples. Some of the network prediction scatter in Figure 8 may be attributed to this difference in the sample preparation procedure.

COMPARISON WITH EMPIRICAL EQUATIONS

Basma and Tuncer [7] proposed two relationships for evaluation of the collapse potential, derived from the statistical regression analysis of test results, given by:

$$CP = 48.496 + 0.102C_u - 0.457w - 3.533\gamma_d + 2.80 \ln P_w, \quad (9)$$

and:

$$CP = 47.506 - 0.072(S - C) - 0.439w - 3.123\gamma_d + 2.851 \ln P_w, \quad (10)$$

where:

$CP =$	collapse potential (%),
$C_U =$	coefficient of uniformity,
$w =$	initial water content (%),
$\gamma_d =$	initial dry unit weight (kN/m^3),
$P_w =$	pressure at inundation (kPa),
$(S - C) =$	difference between the sand and clay percentage.

Predictions of test results based on these equations are shown in Figures 9 and 10, respectively. The relative accuracy of Equations 9 and 10 for prediction of the collapse potential is presented in Table 6. It is clear from Table 6 and Figures 9 and 10 that the aforementioned equations have very poor accuracy compared to the neural network results.

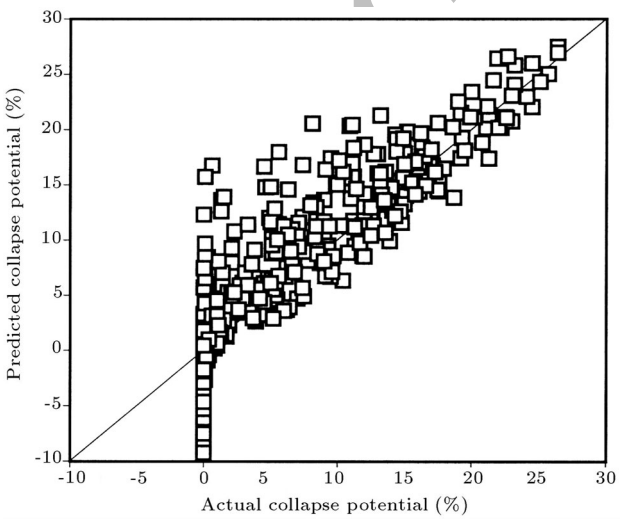

Figure 9. Prediction of collapse potential based on Equation 9.

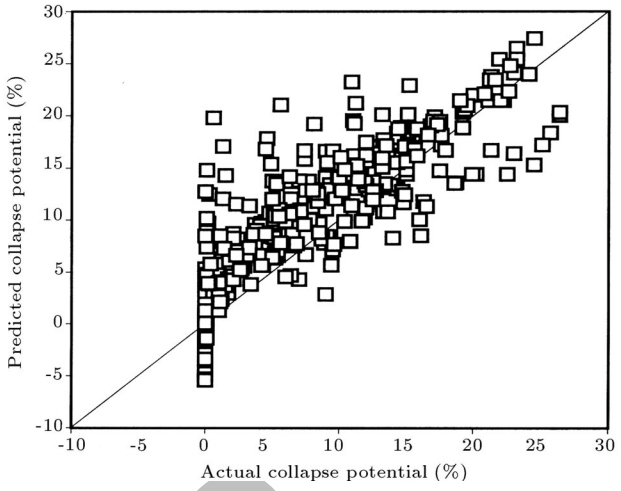

Figure 10. Prediction of collapse potential based on Equation 10.

PARAMETRIC STUDIES

In order to study the influence of different parameters on the amount of collapse potential, the network BPNN6 was tested by a set of input parameters. This set of parameters were as follows: sand content = 13%, silt content = 75%, clay content = 12%, uniformity coefficient = 16.7, coefficient of concavity = 1.4, liquid limit = 22.6, plasticity index = 5, initial water content = 4.9%, initial dry unit weight = 13.6 kN/m^3 and pressure at wetting = 100 kPa. The network prediction was obtained by varying a single parameter each time while keeping all the other parameters constant. The influence of initial dry density, initial water content and the pressure at wetting on collapse potential are shown in Figures 11 to 13, respectively. As expected, Figure 11 indicates that the collapse potential decreases rapidly with an increase in the initial dry unit weight.

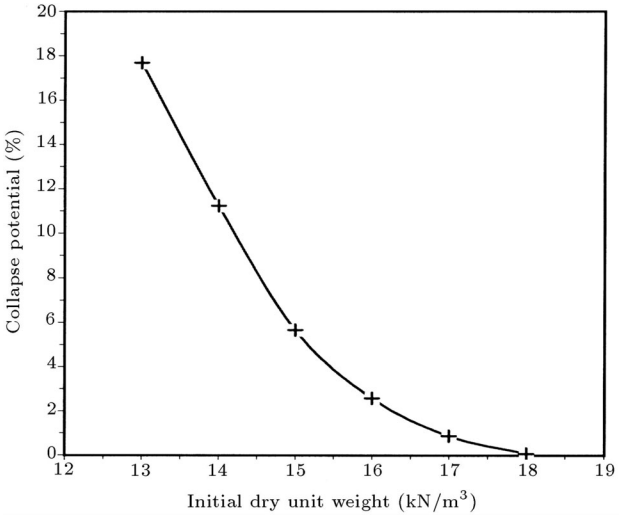

Figure 11. Influence of initial dry unit weight on collapse potential (BPNN6).

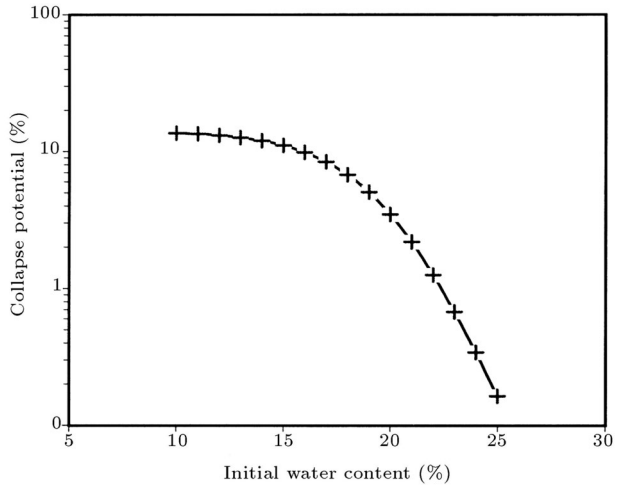

Figure 12. Influence of initial water content on collapse potential (BPNN6).

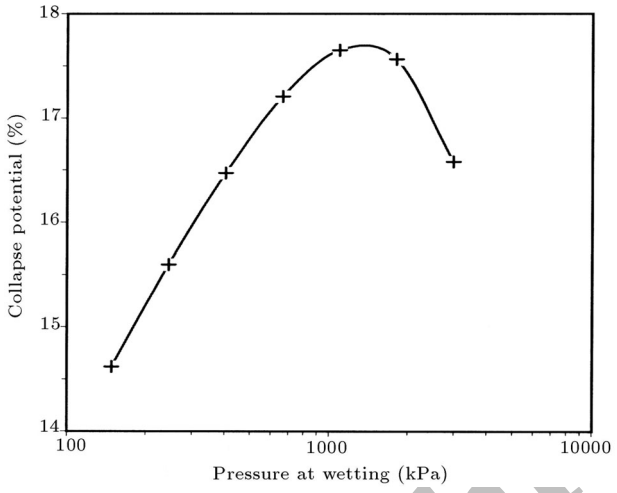

Figure 13. Influence of pressure at wetting on collapse potential (BPNN6).

Figure 12 indicates the dependence of collapse potential on the initial water content. It is interesting to note the similarity in shape between this curve and typical soil water characteristic curves, which relate soil suction (pF) to soil water content. A logarithmic scale was used for the vertical axis in Figure 12, purposely, to be comparable with soil suction (pF) commonly expressed in logarithmic form. In other words, Figure 12 implicitly indicates dependence of the collapse potential on soil suction, that is, collapse potential is higher at high suction values (low water content) and reduces rapidly with an increase in water content. However, any further conclusion on the relationship between Figure 12 and a soil water characteristic curve needs substantial additional investigation. From Figure 13 it can be concluded that the collapse potential increases with an increase in applied pressure up to a "critical" pressure and it is reduced afterwards. This behavior is expected, since pressure at wetting has a dual effect on the collapse potential. On the one hand, it increases the shear stress in the clay bridges between particles which results in subsequent shear failure of these bonds upon saturation. On the other hand, shear failure of these bonds occurs before saturation if loading exceeds a critical value. This kind of behavior has also been reported by other investigators, such as Booth [3].

In order to study the influence of soil composition on the collapse, the silt content was varied, incrementally, from 55% to 85%, while decreasing the clay content by the same amount from 32% to 2% and fixing the sand fraction at 13%. The results shown in Figure 14 indicate that the collapse potential increases with an increase in silt content. Conversely, it may be concluded from the same figure that an increase in clay content accompanied by a decrease in silt content will reduce the collapse potential.

Garson [29] proposed a procedure to determine the relative importance of various input parameters for a neural network by examining the connection weights. This goal was achieved by partitioning the weights of the output layer into components associated with each input parameter. In other words, the net contribution of each input parameter to the resulting output is assessed. Based on this procedure, the relative importance, RI, of input parameters was evaluated and the results, together with connection weights, are shown in Table 7. The results indicate that for a given soil, (that is, for given soil indices, Atterberg limits and gradation characteristics) initial dry unit weight, γ_d, is the most important factor, followed by pressure at wetting and initial water content. From the same table, it may be concluded that the soil properties influencing collapse potential are, ranked on a descending order of importance, Atterberg limits (liquid and plastic limits) followed by coefficient of uniformity and clay content. Coefficient of curvature, C_C, is the least important factor.

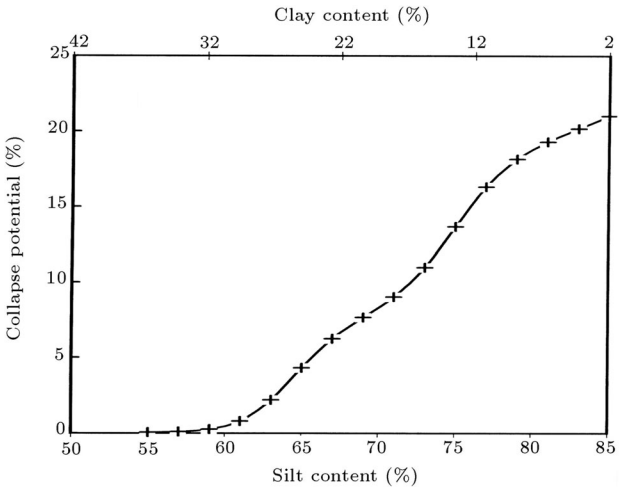

Figure 14. Influence of silt content on collapse potential.

SUMMARY AND CONCLUSION

Collapse potential was evaluated using three different types of neural network (BPNN, RNN and GRNN). Single oedometric test results were used to train and test the network. A large number of sets of data obtained in this study, as well as experimental results reported by other investigators, were used for this purpose. The capability of the neural networks to predict collapse potential was evaluated and compared with each other, as well as with some other relationships available in the literature. Although the results indicate a definite superiority in the neural network approach, in terms of accuracy of prediction of collapse potential, there is still room for further improvement if a standard procedure for preparing the soil sample and testing unsaturated soils in an oedometer apparatus were set forth and followed by different investigators.

Furthermore, the influence of various soil parameters on collapse potential was discussed. From the results, it was concluded that the collapse potential increases with decreasing initial dry density and water content. The collapse increases with the applied pressure up to a critical pressure after which the collapse potential decreases with further increase in the applied pressure. The silt content seemed to play an important role in the collapse potential, since any increase in the amount of silt content showed higher collapse potential.

By analyzing the network connection weights, the relative importance of different parameters on collapse potential was assessed. Based on this analysis, for a given soil type, the initial dry unit weight, γ_d, is the most important factor influencing collapse potential followed by pressure at wetting and initial water content. It was also concluded that the relative importance of soil properties affecting collapse potential, in a descending order, are Atterberg limits (liquid and plastic limits) followed by coefficient of uniformity and clay content. Coefficient of curvature, C_C, is the least important factor. The proposed network is, therefore, a suitable tool to assess different placement conditions (initial dry density and placement water content), as well as stress levels on collapse potential for a given soil. On the other hand, the network may be used to assess the effectiveness of a soil improvement procedure on collapse potential by performing an appropriate parametric study.

Future work is encouraged in the following areas:

1. Setting a standard procedure for sample preparation and testing of compacted soils in a single oedometer test to arrive at more consistent and comparable data;
2. All the results used in this study were confined to soils exhibiting collapse potential. Therefore, the network results are not suitable for soils showing both collapse and swell potential. Hence, expanding the database to include more soil types and a wider range of initial conditions to cover both swell and collapse potential is recommended;
3. Research is also encouraged toward similar work for evaluating the collapse potential of natural soil deposits.

ACKNOWLEDGMENT

The authors wish to express their gratitude to Professor Rob Davis, Department of Civil Engineering, University of Canterbury, New Zealand, for his critical review of the manuscript.

REFERENCES

1. Jennings, J.E., and Burland, J.B. "Limitations to the use of effective stresses in partly saturated soils", *Geotechnique*, **12**(2), pp 125-144 (1962).
2. Lawton, E.C., Fragaszy, R.J. and Hardcastle, J.H. "Collapse of compacted clayey sand", *J. Geotech. Engrg, ASCE*, **115**(9), pp 1252-1267 (1989).
3. Booth, A.R. "The factors influencing collapse settlement in compacted soils", *Proc. Sixth Regional Conf. for Africa on Soil Mechanics and Foundation Engineering*, South African Institute of Civil Engineers, **2**, pp 57-63 (1975).
4. Barden, L., McGown, A., and Collins, K. "The collapse mechanism in partly saturated soil", *Engrg. Geol.*, **7**(1), pp 49-60 (1973).
5. Alwail, T. "Mechanism and effect of fines on the collapse of compacted sandy soils", Ph.D. Thesis, Washington State Univ., Pullman, Washington (1990).
6. Dudley, J.H. "Review of collapsing soils", *J. Soil Mech. Found. Div., ASCE*, **96**(3), pp 925-947 (1970).
7. Basma, A.A. and Tuncer, E.R. "Evaluation and control of collapsible soils", *J. Geotech. Engrg., ASCE*, **118**(10), pp 1491-1504 (1992).
8. Nwabuokei, S.O. and Lovell, C.W. "Compressibility and settlement of compacted fills", *Consolidation of Soils, ASTM*, R.N. Yong and F.C. Townsend, Eds., pp 184-202 (1986).
9. Jennings, J.E. and Knight, K. "The prediction of total heave from the double oedometer test", *Transactions, Symp. on Expansive Clays*, South African Institution of Civil Engineers, pp 13-19 (1957).
10. Houston, S.L., Houston, W.N. and Spadola, D.J. "Prediction of field collapse of soils due to wetting", *J. Geotech. Engrg Div. ASCE*, **114**(1), pp 40-58 (1988).
11. Leonard, G.A. and Davidson, L.W. "Reconsideration of failure initiating mechanisms for Teton dam", *Proc. Int. Conf. on Case Histories in Geotechnical Engineering*, **2**, pp 1103-1113 (1984).

12. Peterson, R. and Iverson, N.L. "Study of several low earth dam failures", *Proc. Third Int. Conf. on Soil Mech. and Found. Engrg.*, **2**, pp 273-276 (1953).
13. Lawton, E.C., Fragaszy, R.J. and Hetherington, M.D. "Review of wetting-induced collapse in compacted soil", *J. Geotech. Engrg, ASCE*, **118**(9), pp 1376-1397 (1992).
14. Ghaboussi, J. "Potential applications of neuro-biological computational models in geotechnical engineering", *Numerical Models in Geotechnics*, G.N. Pande and S. Pietruszezak, Eds., Balkema, Rotterdam, The Netherlands, pp 543-555 (1992).
15. Goh, A.T.C. "Seismic liquefaction potential assessed by neural networks", *J. Geotech. Engrg., ASCE*, **120**(9), pp 1467-1480 (1994).
16. Ellis, G.W., Yao, C., Zhao, R. and Penumadu, D. "Stress-strain modeling of sands using artificial neural networks", *J. Geotech. Engrg., ASCE*, **121**(5), pp 429-435 (1995).
17. Goh, A.T.C. "Neural networks modeling of CPT seismic liquefaction data", *J. Geotech. Engrg., ASCE*, **122**(1), pp 70-73 (1996).
18. Ghaboussi, J. and Sidarta, D.E. "New nested adaptive neural network (NANN) for constitutive modeling", *Computers and Geotechnics*, **22**(1), pp 29-52 (1998).
19. Habibagahi, G., Katebi, S. and Johari, A. "A neural network framework for unsaturated soils", *Proc. of the Asian Conf. on Unsaturated Soils, UNSAT-ASIA 2000*, Singapore, pp 107-111 (2000).
20. Zhu, J.H., Zaman, M.M. and Anderson, S.A. "Modeling of soil behavior with a recurent neural networks", *Can. Geotech. J.*, **35**, pp 858-872 (1998).
21. Abu Kiefa, M.A. "General regression neural network for piles in cohesionless soils", *J. Geotech. and Geoenv. Engrg., ASCE*, **124**(12), pp 1177-1185 (1998).
22. Penumadu, D. and Zhao, R. "Triaxial compression behavior of sand and gravel using artificial neural network", *Computers and Geotechnics*, **24**, pp 207-230 (1999).
23. Bose, N.K. and Liang, P., *Neural Network Fundamentals with Graphs, Algorithms, and Applications*, McGraw Hill Inc., New York (1996).
24. Haykin, S., *Neural Networks: A Comprehensive Foundation*, Prentice Hall Inc., Upper Saddle River, New Jersey (1999).
25. Rumelhart, D.E., Hinton, G.E. and Williams, R.J. "Learning internal representations by error propagation", *Parallel Distributed Processing*, **1**, MIT Press, Cambridge, MA, pp 318-362 (1986).
26. Habibagahi, G. and Mokhberi, M. "A hyperbolic model for volume change behavior of collapsible soils", *Canadian Geot. J.*, **35**(2), pp 264-272 (1998).
27. Lutengger, A.D. and Saber, R.T. "Determination of collapse potential of soils", *Geotech. Testing J.*, **GT6006 11**(3), pp 173-178 (1988).
28. Yeh, Y.C., Kuo, Y.H. and Hsu, D.S. "Building KBES for diagnosing PC pile with artificial neural network", *J. of Comp. Civil Engrg, ASCE*, **7**(1), pp 71-93 (1993).
29. Garson, D.G. "Interpreting neural network connection weights", *AI Expert*, **6**(7), pp 47-51 (1991).